ARTICLE

Detection of Polynuclear Zirconium Hydroxide Species in Aqueous Solution by Desktop ESI-MS

Takayuki SASAKI[1,*], Osamu NAKAOKA[1], Ryuichi ARAKAWA[2],
Taishi KOBAYASHI[1], Ikuji TAKAGI[1] and Hirotake MORIYAMA[1]

[1]*Department of Nuclear Engineering, Kyoto University, Yoshida-honmachi, Sakyo-ku, Kyoto 606-8501, Japan*
[2]*Kansai University, Department of Chemistry and Materials Engineering, Suita, Osaka 564-8680, Japan*

The direct detection of polymerized tetravalent zirconium hydroxides was performed by using a commercially available desktop electrospray ionization mass spectrometry device equipped with a nano-spray capillary heated at 90°C. It was confirmed that the abundance ratio of the species did not depend significantly on the desolvation line temperature up to 170°C. Under the acidic pH condition, the positively charged polymers up to 12-mer species of zirconium were assigned based on the m/z values and the natural abundance isotopic compositions of Zr and Cl. The distribution of the species was observed to change depending on the pH value and the aging period. The hydrolysis constants for the polynuclear species predominantly formed in a solution were estimated from the results of the analysis of the observed spectra with the help of an electrostatic hard sphere model. The obtained values were found to be comparable with the literature ones.

KEYWORDS: zirconium, polymer, ESI-MS, hydrolysis constants

I. Introduction

In the safety assessments of radioactive waste disposal under anaerobic conditions, reliable thermodynamic data of the hydrolysis constants and solubility products are needed to predict the migration behavior of tetravalent long-lived radionuclides, such as actinides, Zr, and Tc. In the case of Zr, only mononuclear species were considered in some early studies of hydrolysis constants,[1,2] but the formation of poly-nuclear and colloidal species was observed in many studies.[3–6] For instance, measuring the size distributions of such species by ultrafiltration (at 3 kDa), Sasaki *et al.* proposed that mononuclear, polynuclear, and colloidal species coexist in weakly acidic and neutral pH solutions.[7] On the other hand, Cho *et al.* developed a method by combining laser-induced breakdown detection (LIBD) with slow coulometric titration in order to sensitively detect the formation of tiny zirconium colloids (>5 nm in size) without the ultrafiltration process.[8] They detected a certain point corresponding to the formation of a ~5 nm compound, which they regarded as the solubility limit. A careful review of the literature on Zr was made by OECD/NEA, and it was proposed that the stability field distributions of the mononuclear and polynuclear hydrolysis species of Zr in 1 M $NaClO_4$ were functions of the total Zr concentration and pH_c.[9] However, the selected species are still limited due to the lack of reliable experimental data. Some modelling studies of the hydrolysis and complexation constants of tetravalent ions were also made.[10–12] Systematic trends of the mononuclear and poly-nuclear hydrolysis constants of tetravalent actinide ions were successfully reproduced by using the hard sphere model.[10] The model was then applied to predict the polynuclear hydrolysis constants of tetravalent zirconium,[13] and the validity of the predictions was shown.

Recently, in order to distinguish different polynuclear species directly, electrospray mass spectrometry (ESI-MS) has been used in the hydration studies of divalent and trivalent metal ions.[14,15] Moulin *et al.* applied the ESI-MS/MS to the investigation of hydroxothorium monomeric species, namely, Th^{4+}, $Th(OH)^{3+}$, $Th(OH)_2^{2+}$, and $Th(OH)_3^+$, by varying the pH in an earlier study.[16] Recently, Walther *et al.* have reported more than 30 polymeric species, including the pentamer of thorium, using the ESI-TOF-MS.[17] They also investigated the distribution of zirconium species by high-resolution TOF-MS, which made it possible to assign the chemical composition by means of the isotopic patterns for the natural isotopic abundances of the Zr and Cl atoms for each mass spectrum. They detected the formation of not only the mononuclear species but also the discrete mass peaks corresponding to the tetramers, pentamers, octamers, and larger polymers. Some results were obtained to show a clear correlation between the peak intensity and concentration of the species, as estimated from an existing thermodynamic database, showing its potential to investigate the equilibriums in a solution quantitatively.

In the present study, a simple, desktop ESI-MS system was used for the measurement of the polynuclear hydrolysis

---

species in the Zr(IV)-OH system, which were suggested to be present by various experimental and theoretical approaches. The nanospray capillaries and heat block installed in the instrument were used for the effective desolvation of moist droplets. The positive ionic complexes were assigned based on the natural abundance isotopic compositions of Zr and Cl. The pH_c and aging period dependences of the distributions of the monomeric and polymeric species were investigated, together with the effect of the heating of the desolvation line on the polymerization. From the MS peak ratios, the hydrolysis constants were evaluated for comparison with the reported values.

II. Experimental Procedure

The mass spectrometric measurements were recorded in the positive ion mode using an LCMS-QP8000 single quadrupole mass analyzer (Shimadzu, Japan). For the purpose of the present study, the liquid chromatography unit was dismounted. The nanospray interface was hand-made in the laboratory and equipped with Au/Pd-coated borosilicate spray capillaries (ES381, Proxeon, Denmark). A small aliquot of Zr sample solution was placed directly inside the emitter, which was mounted on a three-dimensional mechanical stage to adjust the optimum position for emission. A sample solution was sprayed at the tip of a needle, to which a voltage that was 556 V higher than that of a counter electrode was applied. The distance between the needle and the counter electrode was 2 mm, indicating that the externally applied voltage was $2.8 \text{ kV} \cdot \text{cm}^{-1}$. The flow rate of the solution was several tens of nanoliters per min. The so-called curtain gas flowing between the needle and the capillary electrode to aid the desolvation of the charged droplets sprayed was not used. Alternatively, the temperature of the desolvation line was controlled between room temperature and 170°C. The mass spectrometer was calibrated in the positive ion ESI mode using a mixture of polyethylene glycol (PEG) and ammonium adducts. The spectra for the samples were acquired over a mass range of $m/z = 100$–1,500, with an integration time of 4 h.

The $ZrCl_4$ (Aldrich, 99.9%) reagent was used as purchased with no additional purification. The reagent was diluted by HCl solution at a definite pH_c in a polypropylene tube, and its total amount was controlled to be 0.01 $\text{mol} \cdot \text{dm}^{-3}$ (M). No additional electrolyte, such as NaCl, was used to control the ionic strength (I), since the tip of the capillary might have been choked by precipitation of the salt. To investigate the pH dependence, the proton concentration of the aged sample solutions ($pH_c = -\log [H^+]$) was controlled within the range of 0–2.1. The combination glass electrode was calibrated against standard solutions of 0.1/ 0.01 M HCl and NaOH. Immediately after the preparation of the solution, the hydrolysis reaction and polymerization process began, depending on the pH and the aging period.[7] Samples aged for 3 months were used for measurements unless otherwise stated. The spectrum of the samples aged at $pH_c > 3$ could not be obtained due to the low Zr solubility. Considering the effect of a volatile solvent, such as methanol, on a compound at reversible reaction equilibrium, no

additional solvent was used to promote the evaporation of the droplets in the present study.

III. Results and Discussion

1. pH Dependence of Detected Species

The ESI mass spectra of zirconium solutions ($[Zr] = 10^{-2} \text{ mol} \cdot \text{dm}^{-3}$) are measured under different pH_c conditions. The complex species corresponding to each peak is assigned by considering the natural abundances of Zr and Cl. All of the periodical peaks at the interval of $\Delta m/z = 18$ in **Fig. 1** are caused by a difference in the number of water molecules, since the formal charge of the complexes is $+1$. The four major peaks shown in Fig. 1(a) are assigned to the mono-, di-, tri-, and tetramer species of zirconium on the basis of mass distribution. The peak at $m/z = 1,000$–1,100, which might be of the pentamer species, was not clearly assigned due to the peak's broadness and the high background. Figure 1 shows the spectrum for $pH_c = 0.05$ and 90°C, enlarged at $m/z = 193$–203. The mass resolution value is typically $m/\Delta m = 400$ and is much lower than that of common TOF-MS. Also, there is no distinguishable difference between $(H_2^{16}O + {}^{16}OH)$ and $({}^{35}Cl)$ in the spectra. In spite of these limitations, however, the peaks are clearly identified, considering the natural isotopic compositions of ${}^{35}Cl$ and ${}^{37}Cl$. For example, the mass spectrum in Fig. 1 is assigned not to be of $[Zr(OH)_2(H_2O)_2 \cdot Cl]^+$ but of $[Zr(OH)_3(H_2O)_3]^+$ with the natural isotopic compositions of ${}^{90}Zr$, ${}^{91}Zr$, ${}^{92}Zr$, ${}^{94}Zr$, and ${}^{96}Zr$, where the bar graph represents the theoretical mass abundance. In fact, it can be seen in this figure that the fitting becomes worse for $[Zr(OH)_2(H_2O)_2 \cdot Cl]^+$. In a similar manner, the dimer and trimer species shown in Fig. 1 are identified to be of $[Zr_2(OH)_5(H_2O)_3 \cdot Cl_2]^+$ and $[Zr_3(OH)_{11}(H_2O)_3]^+$, respectively.

In similar acidic solutions, Walther *et al.* applied the ESI-TOF-MS to measure Zr hydroxide complexes, in which $ZrOCl_2$ was dissolved.[17] Although a different starting material was used, the zirconium ion would not be present as "yl" ions but Zr^{4+}, as suggested in the literature.[18,19] A mild ESI condition was applied by taking very low declustering conditions, including a low flow rate for the nitrogen curtain gas without heating, and a low electric field between the capillary and the sampling plate. As a result, it was successful to make a complex ion with a number of water molecules remaining in the solvated shell. Under their experimental conditions ($[Zr] = 1.5 \times 10^{-3}$–$1.0 \times 10^{-2} \text{ mol} \cdot \text{dm}^{-3}$ and pH_c 0–3) similar to those of the present study, the typical tetramer complex ions were found to be $[Zr_4(OH)_9(H_2O)_n \cdot Cl_6]^+$ (or $[Zr_4(OH)_9Cl_6]^+ \cdot nH_2O$) and $[Zr_4(OH)_9(H_2O)_n \cdot Cl_5]^{2+}$ (or $[Zr_4(OH)_9Cl_5]^{2+} \cdot nH_2O$), which contained several chloride ions. On the other hand, considering the fingerprint of the isotopic composition in the present study, the spectra in Fig. 1 may be assigned to $[Zr_4(OH)_{14}(H_2O)_7 \cdot Cl]^+$, rather than to $[Zr_4(OH)_9(H_2O)_2 \cdot Cl_6]^+$ in the above species. This difference may be attributed to different ESI conditions, especially to different desolvation temperatures. As their EXAFS study has suggested that the zirconium in the solution is surrounded by oxygen atoms under the present experimental conditions,[17] by assuming the same original spe-
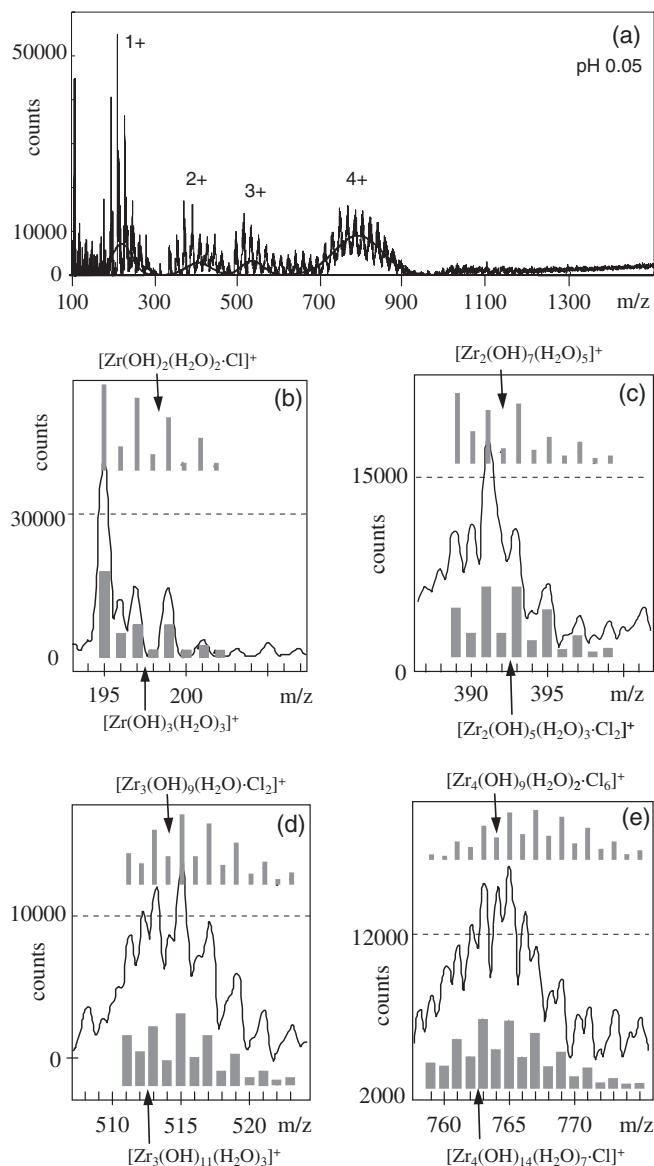
Fig. 1 ESI mass spectra in positive ion mode of Zr solution at pH_c of 0.05. The overview spectrum (a) is shown with the solid lines of Gaussian curve fitting. The signs of $i+$ indicate $[i\text{-mer}]^+$ species ($i = 1$–4). The annotated spectra show monomer (b), dimer (c), trimer (d), and tetramer (e) species, respectively. The experimental spectra for specific complex ions are compared with the simulated isotopic patterns given in a gray bar graph. The bottom pattern for the indicated composition formula is likely assigned, while the top one is an example of the mismatches.

cies of $[Zr_4(OH)_8(H_2O)_n \cdot Cl_7]^+$ in the presence of dilute hydrochloric acid, the following reactions are considered to occur in the ESI processes since the neutral molecules of not only H_2O but also HCl may be evaporated at higher temperatures.

$$[Zr_4(OH)_8(H_2O)_n \cdot Cl_7]^+$$
$$\rightarrow [Zr_4(OH)_9(H_2O)_{n'} \cdot Cl_6]^+ + (n - n' - 1)H_2O + HCl$$
$$[Zr_4(OH)_8(H_2O)_n \cdot Cl_7]^+$$
$$\rightarrow [Zr_4(OH)_{14}(H_2O)_7 \cdot Cl]^+ + (n - 13)H_2O + 6HCl$$
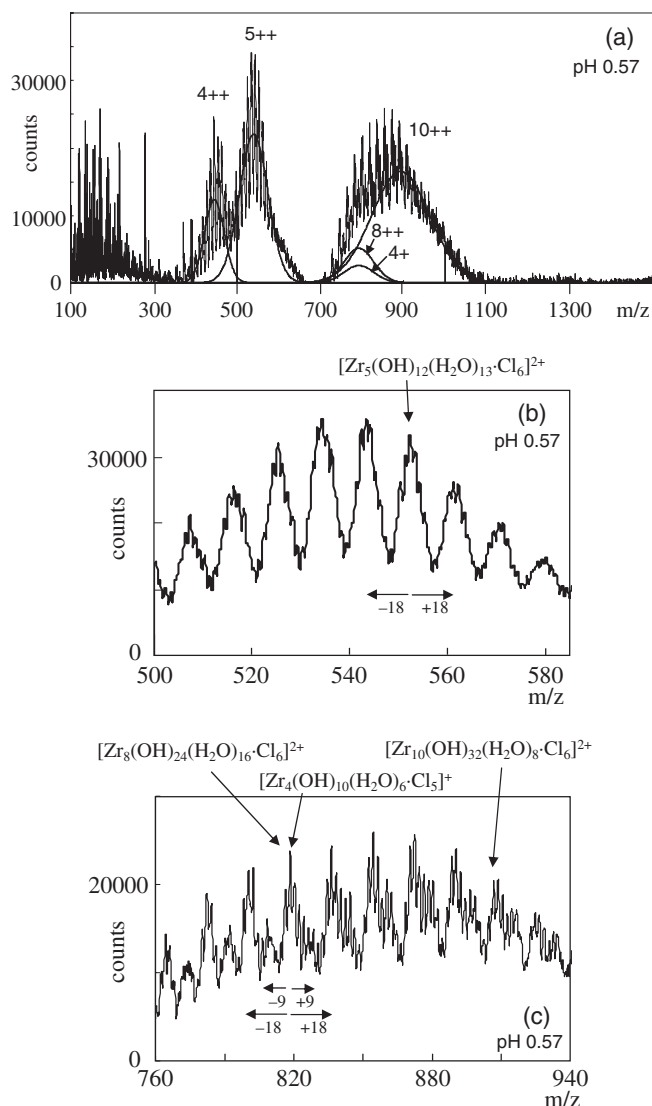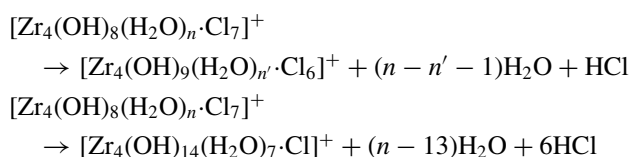
Fig. 2 ESI mass spectra of Zr solution at pH_c of 0.57. The overview spectrum (a) is shown with the solid lines of Gaussian curve fitting. The signs of $i+$ and $i++$ indicate $[i\text{-mer}]^+$ and $[i\text{-mer}]^{2+}$ species, respectively. The peak clusters between m/z = 500–585 and 760–940 are magnified in (b) and (c), respectively.

As in the case of the evaporation of H_2O, only the evaporation of a small amount of HCl may occur under the mild conditions adopted by Walther *et al.*, while the evaporation of a large amount of HCl may occur in the present ESI process at 90°C. It is noted here that the presently observed species of $[Zr_4(OH)_{14}(H_2O)_7 \cdot Cl]^+$ is also formed from a different original species of $[Zr_4(OH)_{10}(H_2O)_n \cdot Cl_5]^+$ as

$$[Zr_4(OH)_{10}(H_2O)_n \cdot Cl_5]^+$$
$$\rightarrow [Zr_4(OH)_{14}(H_2O)_7 \cdot Cl]^+ + (n - 11)H_2O + 4HCl.$$
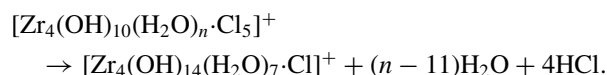
Thus, a careful consideration is needed for the analysis of the assigned species, as is given later.

In the spectrum at pH_c of 0.57 (**Fig. 2**), positive divalent species were observed in the low m/z range, which were the tetramer and pentamer at m/z = 450 and 550, respectively. Since the peaks observed at m/z < 300 were not attributed to zirconium species, they were excluded from the spectrum
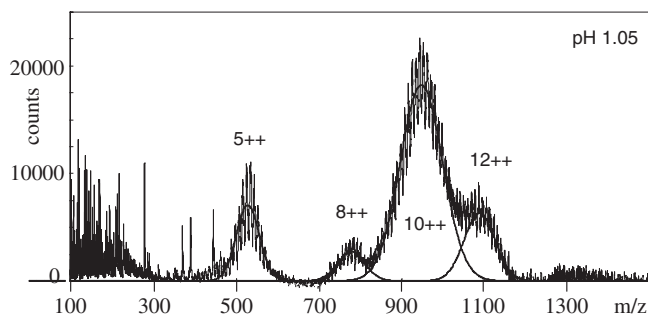
Fig. 3 ESI mass spectra of Zr solution at pH_c of 1.05. The solid lines represent Gaussian curve fitting for [i-mer]$^{2+}$ species abbreviated to i++.
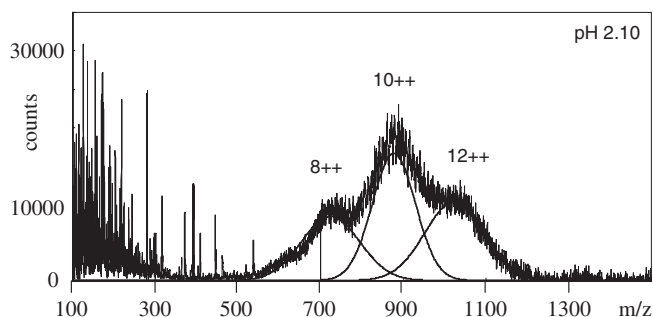

Fig. 4 ESI mass spectra of Zr solution at pH_c of 2.10. The solid lines represent Gaussian curve fitting for [i-mer]$^{2+}$ species abbreviated to i++.

analysis. On the other hand, the magnified spectra at around m/z = 550 and 850 (Fig. 2) were assigned to be of the divalent species such as [Zr$_5$(OH)$_{12}$(H$_2$O)$_{13}$·Cl$_6$]$^{2+}$ (m/z = 553), [Zr$_8$(OH)$_{24}$(H$_2$O)$_{16}$·Cl$_6$]$^{2+}$ (m/z = 819) and [Zr$_{10}$(OH)$_{32}$(H$_2$O)$_8$·Cl$_6$]$^{2+}$ (m/z = 907), considering the interval of Δm/z = 18/2 = 9, with which the tetramer (1+, Δm/z = 18), such as [Zr$_4$(OH)$_{10}$(H$_2$O)$_6$·Cl$_5$]$^+$ (m/z = 821), might partly overlap. Thus, no monovalent species of the pentamer, octamer, and 10-mer were observed, while both monovalent and divalent species were observed for tetramers.

In **Fig. 3**, at pH_c of 1.05, it is noteworthy that all of the monovalent species disappear and larger species of the 10-mer and 12-mer, such as [Zr$_{12}$(OH)$_{40}$(H$_2$O)$_{12}$·Cl$_6$]$^{2+}$ (m/z ∼ 1101), are newly observed in the present study. In particular, the 12-mer would be the first species detected by the ESI-MS method. At the higher pH_c of 2.10 (**Fig. 4**), where the apparent solubility decreases, the minor peaks for the tetramer and pentamer were hardly distinguished.

2. Temperature Effect in ESI Process

As described above, heating the injection line to 90°C was effective for the desolvation of the species. However, there was a concern that an undesirable decomposition and/or polymerization might occur. A 0.01 M zirconium sample solution at pH_c of 0.05 was used for the measurement of such secondary reactions. Only water cluster peaks could be observed at 70 and 80°C, while no significant peak appeared
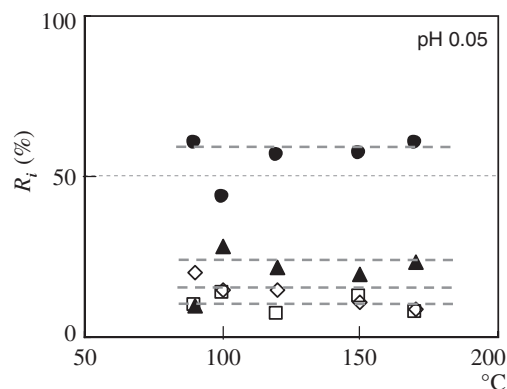

Fig. 5 Effect of the desolvation line temperature on the zirconium polymer distribution at pH_c of 0.05. The symbols ◇, □, ▲, and ● show mono-, di-, tri-, and tetramer species, respectively. The error in the R_i values calculated is small relative to the plot size.

at 25°C. At 90°C, the following typical zirconium complexes with some "associated" water molecules were observed, as shown in Fig. 1: the mono-, di-, tri-, and tetramer species of zirconium. As the temperature increased, no significant change in the peak property was observed, and only the shift of the Gaussian distribution centers was observed at lower m/z positions, as a result of the vaporization of water. The distribution ratios of the four species were calculated from these peak areas and are plotted in **Fig. 5**. Up to the high temperature of 170°C, the ratios seem to remain constant, although some plots are scattered. This suggests that the Zr units bridged by oxide ions seem to be hardly decomposed compared with the associated water molecules. However, a small and broad peak, which corresponds to the species larger than the tetramer, is observed at >150°C. These unidentified species must have been produced in the heated line. Thus, it is preferable to use the mildest condition of 90°C.

3. Sample Aging for Polymerization

The progress of polymerization was investigated in a solution, the pH_c of which was maintained at 1.54 throughout the experimental period in an argon-filled glove box for up to 1,440 h (2 months). The pentamer, octamer, and 10-mer species were observed in the fresh solution. The ratio of the pentamer then began decreasing, while those of the octamer and 10-mer increased. After one month, the 12-mer species appeared with the growth of the octamer and 10-mer species. This is the first report of the hydrolysis species of the 10- and 12-mer complexes. Peaks at higher m/z positions were observed but could not be identified due to the low S/N counting ratio. The time dependence of the relative abundance is shown in **Fig. 6**. Such a polymerization process was considered to be slow in previous solubility studies.[7,8] For instance, the formations of polynuclear and colloidal species, for which a steady state size distribution was reached after a few months, were observed in oversaturation experiments.[7] From the observed size distributions, it was found that 3 kDa mononuclear, polynuclear, and colloidal species (Microcon Centrifugal Filter, Millipore) might exist even in an acidic solution. It is interesting to note that further
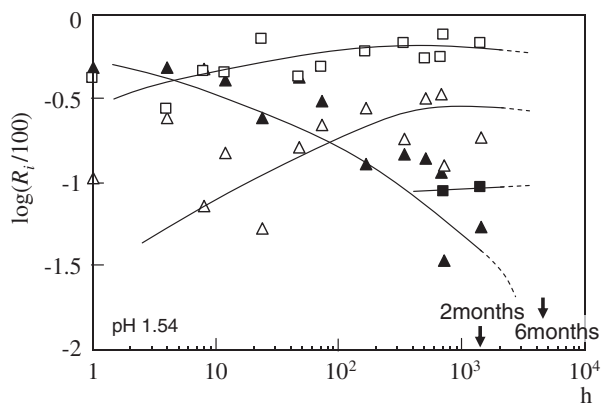
Fig. 6　Aging time dependence of polymerization in the zirconium solution at pH$_c$ of 1.54. The symbols ▲, △, □, and ■ show 5-, 8-, 10-, and 12 mer species, respectively. The error in the R_i values calculated is small relative to the plot size.
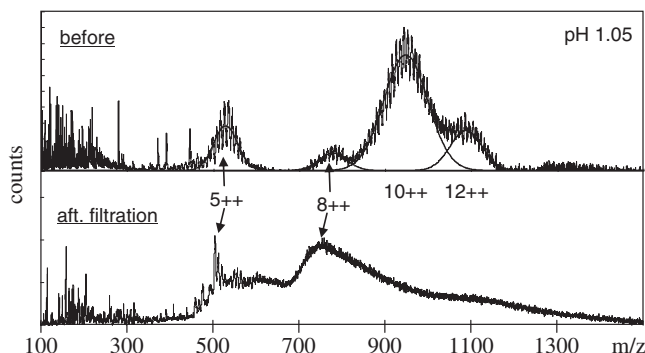

Fig. 7　Comparison of ESI mass spectra obtained before and after 3 kDa (lower) ultrafiltration. The solution is aged for 3 months at pH$_c$ of 1.05.

polymerization would occur very slowly after reaching a nearly steady state in 3 months.

4. Effect of Ultrafiltration on Size Distribution

Because of the use of a 3 kDa sieve mesh ultramembrane filter, corresponding to a size of 2 nm, some zirconium hydrolysis species, such as those smaller than the tetramer (∼2 nm), are considered to pass through. For observation of the effect of ultrafiltration, the ESI-MS spectrum of the filtrated sample solution after aging for 3 months ([Zr]$_{ini}$ = 1×10^{-2} mol·dm^{-3}; pH$_c$, 1.05) was taken together with that of the nonfiltered one, as shown in **Fig. 7**. In the spectrum after filtration, it is seen that the peaks for the 10- and 12-mer considerably decrease in intensity, probably due to the cutoff, and that the 5- and 8-mers still remain in the solution. In other words, the polynuclear species are not clearly cut off by the tetramer species. It is important to take into account this cutoff performance for solubility measurements by ultrafiltration.

5. Apparent Distribution of Species and Hydrolysis Constants

The relative abundance R_i of the zirconium species can be determined from the ESI-MS spectra at 90°C. When the Zr

abundance ratio is assumed to be equal to the ratio of the peak area for a given species to the overall peak area, the abundance ratio of the i-mer ($i \geq 1$) species in a spectrum can be described as

$$R_i(\%) = \frac{[peak\ area\ for\ i\text{-}mer\ species]}{\sum [peak\ area\ for\ n\text{-}mer\ species]} \times 100, \quad (1)$$

where n and i represent the degree of polymerization, *i.e.*, the number of Zr units in each species. The overlapping peaks in a given m/z range are analyzed as follows. In the analytical formulation, the spectrum for each species is assumed to be a simple Gaussian curve, and the peak intensity at a given m/z value, x, is given by

$$Int(x) = \sum_{i=1}^{n} j_i \exp\left[-\frac{(x-k_i)^2}{2l_i^2}\right], \quad (2)$$

where the coefficients j, k, and l are the local maximal intensity, mean, and width for the ith species, respectively. The curve fitting results for the spectra in Figs. 1–4 are summarized in **Table 1**. The numerical integration value for each peak area S_i ($i = 1, 2, 3, 4, 5, 8, 10$, and 12) is evaluated by

$$S_i = \int j_i \exp\left[-\frac{(x-k_i)^2}{2l_i^2}\right]dx = j_i l_i \sqrt{2\pi}. \quad (3)$$

The R_i values in Eq. (1) are calculated by using the S_i values obtained. The results are also summarized in Table 1.

The results of the direct detection of the polynuclear species can be applied to the estimation of hydrolysis constants. As mentioned above, however, it is considered that some H$_2$O and HCl molecules that evaporate from the original solution species though the Zr units bridged by oxide ions are hardly decomposed in the present ESI process. It is thus important to find out the original solution form for each i-mer ($i \geq 1$) species. Our procedure is to take the representative species, *i.e.*, the number of Zr units, which are predominantly formed in the studied pH range by considering available hydrolysis constants and predictions. In the case of mononuclear species in a solution at pH 0, for example, it is expected from available hydrolysis constants that Zr^{4+} or ZrOH^{3+} will be more probably detected than Zr(OH)$_3^+$ in the present study. Also, the polynuclear species given in Table 1 are expected to be more probably detected than the species from the hydrolysis constants obtained by the electrostatic hard sphere model,[10,13] which is extended from the 4-mer to the 12-mer, as given below.

By taking the R_i values in Table 1 and by using the following equations, one can obtain the hydrolysis constants for the estimated original solution species of Zr$_i$(OH)$_q^{4i-q}$.

$$R_i(\%) = ([Zr_i(OH)_q^{4i-q}]/\Sigma[Zr_i(OH)_q^{4i-q}]) \times 100$$
$$= \beta_{i,q}'[Zr^{4+}]^i[OH^-]^q/\Sigma(\beta_{i,q}'[Zr^{4+}]^i[OH^-]^q) \times 100, \quad (4)$$

where $\beta_{i,q}'$ represents the apparent hydrolysis constants,

$$\beta_{i,q}' = [Zr^{4+}]^i[OH^-]^q/[Zr_i(OH)_q^{4i-q}].$$

Then,

$$[Zr]_{ini} = \Sigma\ i[Zr_i(OH)_q^{4i-q}] = \Sigma(i\beta_{i,q}'[Zr^{4+}]^i[OH^-]^q). \quad (5)$$

Table 1 Relative abundance of the zirconium hydroxides determined by Gaussian curve fitting of the spectra in Figs. 1–4

pH$_c$	i, q[a]	charge	R_i (%)	$j \pm \Delta j$	$k \pm \Delta k$	$l \pm \Delta l$
0.05	1, 1	1+	20.2 ± 1.2	7120 ± 190	221 ± 1	24.3 ± 0.8
	2, 4	1+	9.9 ± 1.1	2840 ± 180	405 ± 2	29.9 ± 2.4
	3, 6	1+	9.8 ± 1.0	3260 ± 190	535 ± 2	25.7 ± 1.9
	4, 10	1+	60.1 ± 3.0	9040 ± 140	789 ± 1	56.8 ± 1.1
0.57	4, 10	1+	15.4 ± 1.2[b]	2530 ± 180	794 ± 1	35.6 ± 1.6
	4, 10	2+		12300 ± 220	447 ± 1	23.7 ± 0.6
	5, 12	2+	30.7 ± 1.0	22000 ± 190	541 ± 1	34.4 ± 0.5
	8, 22	2+	7.3 ± 0.3	5070 ± 360	794 ± 1	35.6 ± 1.6
	10, 30	2+	46.5 ± 1.7	16400 ± 160	895 ± 2	69.6 ± 1.5
1.05	5, 12	2+	13.6 ± 0.3	5620 ± 50	529 ± 1	27.9 ± 0.3
	8, 22	2+	6.1 ± 0.3	2180 ± 60	779 ± 1	32.3 ± 1.0
	10, 30	2+	64.2 ± 0.8	14500 ± 60	948 ± 1	51.0 ± 0.3
	12, 38	2+	16.1 ± 0.3	5040 ± 50	1090 ± 1	36.9 ± 0.5
2.10	8, 22	2+	26.9 ± 0.7	8360 ± 50	725 ± 2	70.2 ± 1.1
	10, 30	2+	39.5 ± 1.1	16600 ± 260	878 ± 1	52.1 ± 0.6
	12, 38	2+	33.6 ± 1.1	10200 ± 140	1020 ± 1	71.6 ± 1.6

[a] The values i and q are determined by the assignment of the ESI-MS spectrum and calculation using the hard sphere model, respectively. See the text. [b] Combined value of the species $(4,10)^+$ and $(4,10)^{2+}$.

Equations (4) and (5) are solved simultaneously by considering the effect of ionic strength. The SIT coefficients are taken from the literature or are assumed, as shown in **Table 2**. The results are summarized in Table 2, in which the hydrolysis constants for (1,1) to (12,38) species at zero ionic strength are given by SIT corrections.

6. Electrostatic Hard Sphere Model

In our previous study on tetravalent actinide hydroxides,[10] the formation of a continuous series of polynuclear hydroxide complexes was proposed and the electrostatic hard sphere model was applied to reproduce the systematic trends of the mononuclear and polynuclear hydrolysis constants. This model was also applied to the polynuclear hydrolysis species of Zr(IV) up to tetramers.[13] In the present study, it is extended to include the 12-mer in order to analyze the present results. For the formation of polynuclear species, a polymerization process similar to that for tetravalent actinide ions was assumed by considering the formation of polymers bridged by hydroxide ions (Zr-OH-Zr).[10] For simplicity, the formation of oxygen bridges (Zr-O-Zr) is not taken into account, and the polymer units are assumed to form connected antiprismatic cubes, as shown in **Fig. 8**.

By considering the coulombic interactions between hard spheres, the electrostatic potential energy $E_{i,q}$ of each species is given by

$$E_{i,q} = \sum_{a \neq b}^{N} \left(\frac{Z_a Z_b}{\varepsilon_{dc} d_{ab}} \right), \quad (6)$$

where N denotes the total number of hard spheres in the (i,q) species, Z_a and Z_b are the electric charges of the hard spheres a and b, respectively, ε_{dc} is the dielectric constant, and d_{ab} is the distance between the hard spheres a and b. Taking into account the coordinated water molecules, the hydrolysis reaction for the $(1,q)$ species is given by

| (i,q)	Hydrolysis species	(i,q)	Hydrolysis species
$(1,q)$		$(2,q)$	
$(3,q)$		$(4,q)$	
$(7,q)$			
$(10,q)$			
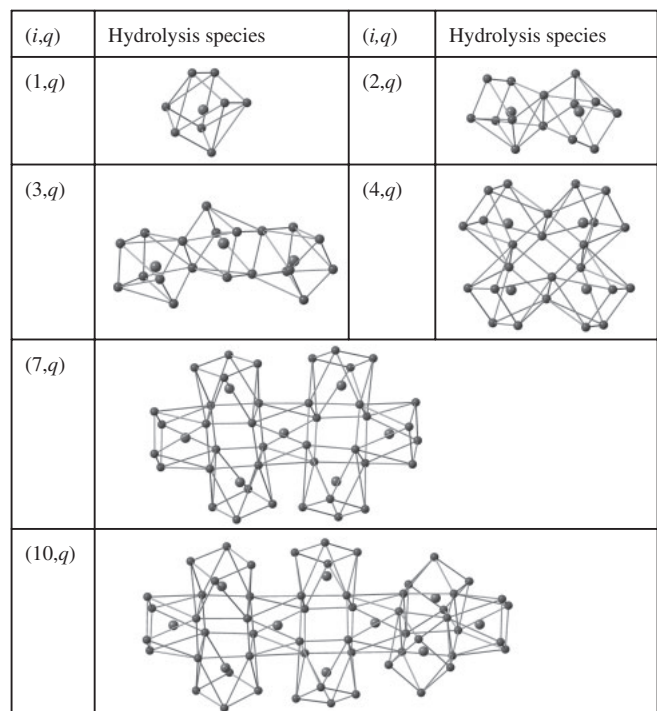
Fig. 8 Chemical structures of i-mer zirconium species assumed in the hard sphere model analysis. All hydrogen atoms in the Zr-OH-Zr bridges, hydroxyl ions, and hydrated water molecules are omitted for simple description.

$$\mathrm{Zr(H_2O)_8^{4+}} + q\mathrm{OH}^- \rightleftharpoons \mathrm{Zr(OH)}_q\mathrm{(H_2O)}_{8-q}^{4-q} + q\mathrm{H_2O}, \quad (7)$$

where each mononuclear species forms an antiprismatic matrix with a central zirconium ion. For the polynuclear species, each zirconium atom is assumed to be in a unit matrix connected to other matrices by a double hydroxyl

Table 2 Equilibrium constants $\log_{10} \beta^\circ_{i,q}$ at zero ionic strength. Calculated values and the SIT coefficients $\varepsilon_{i,Cl}$ were obtained using the hard sphere model

$(i,q)^{4i-q}$	This work	Walther et al.[17]	NEA-TDB[9]	Calcd.	$\varepsilon_{i,Cl}$[b]
$(1,1)^{3+}$	14.29[a)6)]	14.1	14.32 ± 0.22	14.29[a)6)]	0.33[9]
$(1,2)^{2+}$		27.8	28.98 ± 1.06	26.7	0.18[17]
$(1,3)^{+}$		37.1		35.9	0.08[17]
$(1,4)^{0}$				43.1	0[17]
$(1,6)^{2-}$				48[a)13)]	0
$(2,4)^{4+}$	61.8 ± 0.8			59.2	0.33
$(2,6)^{2+}$				85.0	0.18
$(3,4)^{8+}$		55.4	56.4 ± 0.3	53.8	0.18[17]
$(3,6)^{6+}$	91.6 ± 1.2			87.7	0.28
$(3,9)^{3+}$			138.19 ± 0.08		
$(3,10)^{2+}$				138.1	0.18
$(3,12)^{0}$				149.0	0
$(4,8)^{8+}$		117.8	118.52 ± 0.65	123.1	0.5[17]
$(4,10)^{6+}$	154.5 ± 1.3	149		156.9	0.28[17]
$(4,14)^{2+}$				204.1	0.18
$(4,15)^{+}$			222.58 ± 0.24		
$(4,16)^{0}$			232.39 ± 0.80	219.8	0
$(5,11)^{9+}$		165.4			
$(5,12)^{8+}$	182.0 ± 2.3	180		182.0	0.5
$(5,16)^{4+}$		230			
$(7,20)^{8+}$				309.2	0.5
$(7,24)^{4+}$				362.8	0.33
$(8,19)^{13+}$		281.3			
$(8,22)^{10+}$	335.3 ± 2.8	324.5		334.0	3
$(8,24)^{8+}$				367.7	0.5
$(8,27)^{5+}$		385.75			
$(10,30)^{10+}$	457.6 ± 3.3			460.8	3
$(10,38)^{2+}$				560.8	0.18
$(10,40)^{0}$				574.9	0
$(12,38)^{10+}$	575.5 ± 4.0			577.5	3

Calculated values are extended to 5-, 7-, 8-, 10-, and 12-mer species from 4-mer species in Ref. 13), which is bound 4-mer with 3-mer species in the geometry of each distorted square antiprism, as shown in Fig. 8. [a)]Fixed parameters and [b)]assumed values in italics.

bridge $-(OH)_2-$, and the hydrolysis reactions for the (i,q) species with $i \geq 1$ are written as

$$i\mathrm{Zr(H_2O)_8^{4+}} + q\mathrm{OH^-}$$
$$\rightleftharpoons \mathrm{Zr}_i(\mathrm{OH})_q(\mathrm{H_2O})_r^{4i-q} + (8i - r)\mathrm{H_2O}, \quad (8)$$
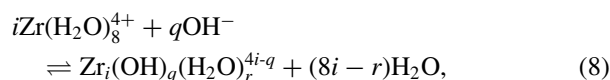
where the number of water molecules in the (i,q) species, r, can be expressed by

$$r = (16i + 8)/3 - q, \quad \text{for } i = 1, 4, 7 \cdots = 3m - 2,$$
$$r = (16i + 10)/3 - q, \quad \text{for } i = 2, 5, 8 \cdots = 3m - 1,$$
$$r = (16i + 12)/3 - q, \quad \text{for } i = 3, 6, 9 \cdots = 3m.$$

The potential energy change ΔE in reaction (8) is then given by

$$\Delta E_{i,q} = E_{i,q} - iE_{1,0} + [(8i - r) - q]E', \quad (9)$$

where $E_{i,q}$ denotes the contribution of $\mathrm{Zr}_i(\mathrm{OH})_q(\mathrm{H_2O})_r^{4i-q}$ to the potential energy change, $E_{1,0}$, the contribution of $\mathrm{Zr(H_2O)_8^{4+}}$, and E', the contribution of a free water molecule released from the hydroxyl bridges. Accordingly, the

standard state hydrolysis constant $\beta^\circ_{p,q}$ of each species is expressed by

$$\beta^\circ_{i,q} = \exp(-\Delta E_{i,q}/RT), \quad (10)$$

where R and T denote the gas constant and absolute temperature, respectively.

In our previous study, by considering the reference values of $\log \beta^\circ_{1,1}$, $\log \beta^\circ_{1,6}$, and $\log \beta^\circ_{4,8}$, and using Eqs. (6), (9), and (10), the parameter values of the electric charge of water molecules Z_{H2O}, ε_{dc}, and the E' value were determined to be -0.066, 25.7, and 18.8 kJ·mol^{-1}, respectively. In the calculation, the electric charge of $\mathrm{Zr^{4+}}$ ions, Z_{Zr}, was assumed to be $+4$ without the contribution of non-electrostatic interactions, and the electric charge of $\mathrm{OH^-}$ ions, Z_{OH}, was assumed to be -1. The ionic radius of $\mathrm{Zr^{4+}}$ in its antiprismatic structure was evaluated to be 0.089 nm by considering the ionic radius of 0.138 nm for $\mathrm{OH^-}$ and $\mathrm{H_2O}$.[10,20,21] These values are adopted in the present study.

Table 2 summarizes the calculated log $\beta_{i,q}$ values for $i = 1$–10. The values obtained by the electrostatic hard sphere model are compared with the values of Walther *et al.*[17] and the OECD-NEA thermodynamic database.[9] There may be some similarities and differences in these values in Table 1. As a cause of slightly high values of log $\beta_{i,q}$ compared with Walther *et al.*'s data, the polymerization to larger species might proceed due to the longer aging period compared with Walther *et al.*'s samples aged for at least 1 h.

For comparison of the values, however, it is noted that the present log $\beta_{i,q}$ values are obtained by assuming such predominant species as (1,1), (2,4), (3,6), (4,10), (5,12), (8,22), (10,30), and (12,38) in the pH$_c$ range of 0.05 to 2.10 in the present study. Because of this assumption, the values are considered to be only temporal, for which further confirmation is needed. In spite of this limitation, the values obtained by the electrostatic hard sphere model are considered to be useful for checking the consistency of the reported experimental values and for predicting the missing values from a systematic point of view.

IV. Conclusions

By using a commercially available and desktop nano-ESI-MS, the direct detection of the polymerized tetravalent zirconium hydroxides was performed. For a quantitative analysis, a careful interpretation of the ESI-MS spectra was needed in the present study, in which the 90°C desolvation line was used. It was confirmed that the abundance ratio of the species did not depend significantly on the desolvation line temperature up to 170°C. Then, the hydrolysis constants for the polynuclear species were obtained from the results of the analysis of the observed spectra with the help of the electrostatic hard sphere model to predict systematically the 'likely' predominant species. The obtained values were found to be comparable to the literature values. It was also found that the polymerization was still going on after aging at a given pH for 3 months. This interesting "*in situ*" observation provided new insights into the phenomena of very slow apparent solubility changes of tetravalent metal hydroxides.

Acknowledgement

References

1) P. N. Kovalenko, K. N. Bagdsarov, "The solubility of zirconium hydroxide," *Russ. J. Inorg. Chem.*, **6**, 272 (1961).

2) H. Bilinski, M. Branica, L. G. Sillen, "Preparation and hydrolysis of metallic ions. II. Studies on the solubility of zirconium hydroxide in dilute solutions and 1 M NaClO$_4$," *Acta Chem. Scand.*, **20**, 853 (1966).

3) A. J. Zielen, R. E. Connick, "The hydrolytic polymerization of zirconium in perchloric acid solutions," *J. Am. Chem. Soc.*, **78**, 5785 (1956).

4) G. M. Muha, P. A. Vaughan, "Structure of the complex ion in aqueous solutions of zirconyl and hafnyl oxyhalides," *J. Chem. Phys.*, **33**, 194 (1960).

5) A. Veyland, L. Dupont, C. Pierrad, J. Rimbault, M. Aplincourt, "Thermodynamic stability of zirconium(IV) complexes with hydroxy ions," *Eur. J. Inorg. Chem.*, 1765 (1998).

6) C. Ekberg, G. Kallvenius, Y. Albinsson, P. Brown, "Studies on the hydrolytic behavior of zirconium(IV)," *J. Solution Chem.*, **33**, 47 (2004).

7) T. Sasaki, T. Kobayashi, I. Takagi, H. Moriyama, "Solubility measurement of zirconium(IV) hydrous oxide," *Radiochim. Acta*, **94**, 489 (2006).

8) H. Cho, C. Walther, J. Roche, V. Neck, M. A. Denecke, K. Dardenne, Th. Fanghänel, "Combined LIBD and XAFS investigation of the formation and structure of Zr(IV) colloids," *Anal. Bioanal. Chem.*, **383**, 28 (2005).

9) P. Brown, E. Curti, B. Grambow, C. Ekberg, *Chemical Thermodynamics of Zirconium: Chemical Thermodynamics*, F. J. Mompean *et al.* (Eds.), Vol. 8, Elsevier, North-Holland, Amsterdam (2005).

10) H. Moriyama, T. Sasaki, T. Kobayashi, I. Takagi, "Systematics of hydrolysis constants of tetravalent actinide ions," *J. Nucl. Sci. Technol.*, **42**, 626 (2005).

11) V. Neck, J. I. Kim, "Solubility and hydrolysis of tetravalent actinides," *Radiochim. Acta*, **89**, 1 (2001).

12) V. Neck, J. I. Kim, "An electrostatic approach for the prediction of actinide complexation constants with inorganic ligands-application to carbonate complexes," *Radiochim. Acta*, **88**, 815 (2000).

13) T. Sasaki, T. Kobayashi, I. Takagi, H. Moriyama, "Hydrolysis constant and coordination geometry of zirconium(IV)," *J. Nucl. Sci. Technol.*, **45**, 735 (2008).

14) S. E. Rodriguez-Cruz, R. A. Jockusch, E. R. Williams, "Hydration energies and structures of alkaline earth metal ions, M^{2+}(H$_2$O)$_n$, $n = 5$–7, M = Mg, Ca, Sr, and Ba," *J. Am. Chem. Soc.*, **121**, 8898 (1999).

15) A. Sarpola, V. Hietapelto, J. Jalonen, J. Jokela, R. S. Laitinen, "Identification of the hydrolysis products of AlCl$_3$·6H$_2$O by electrospray ionization mass spectrometry," *J. Mass Spectrom.*, **39**, 423 (2004).

16) C. Moulin, B. Amekraz, S. Hubert, V. Moulin, "Study of thorium hydrolysis species by electrospray-ionization mass spectrometry," *Anal. Chim. Acta*, **441**, 269 (2001).

17) C. Walther, J. Rothe, M. Fuss, S. Büchner, S. Koltsov, T. Bergmann, "Investigation of polynuclear Zr(IV) hydroxide complexes by nanoelectrospray mass-spectrometry combined with XAFS," *Anal. Bioanal. Chem.*, **388**, 409 (2007).

18) C. F. Baes, R. E. Mesmer, *The Hydrolysis of Cations*, John Wiley & Sons, New York (1976).

19) D. B. McWhan, G. Lundgren, "Crystal structure of Zr$_2$(OH)$_2$(SO$_4$)$_3$(H$_2$O)$_4$," *Inorg. Chem.*, **5**, 284 (1966).

20) Y. Marcus, *Ion Solvation*, Wiley-Interscience, Chichester (1985).

21) Y. Marcus, "Ionic-radii in aqueous-solutions," *Chem. Rev.*, **88**, 1475 (1988).